Measurement of the temperature dependence of midinfrared optical absorption spectra of germanium in intense laser fields

H. Furuse, N. Mori, H. Kubo, H. Momose, and M. Kondow
Department of Electronic Engineering, Osaka University, Suita City, Osaka 565-0871, Japan
(Received 19 December 2006; revised manuscript received 28 February 2007; published 2 May 2007)

We have investigated the temperature dependence of midinfrared optical absorption in germanium under intense free-electron laser fields. We observed that the absorption decreases as temperature decreases. We find that the temperature dependence of the absorption is consistent with calculations based on the Keldysh theory, in which the temperature dependence of the direct-gap energy of germanium is considered.

DOI: 10.1103/PhysRevB.75.205101 PACS number(s): 78.20.−e, 41.60.Cr, 42.70.Km, 78.30.−j

I. INTRODUCTION

Laser pulse ablation of transparent materials has been the subject of numerous studies.[1–3] It has generally been assumed that photoionization processes, either multiphoton ionization[4] or tunneling ionization,[5] first generate seed electrons. For pulses shorter than the energy relaxation time (typically 10 ps), the laser energy is absorbed by the seed electrons faster than it is transferred to the lattice by electron-phonon coupling. Breakdown of transparent material proceeds via electron avalanche initiated by the seed electrons. When the density of the free electrons exceeds a certain threshold, enough energy is absorbed to produce macroscopic ablation.[6] In this process, however, a definitive answer to several fundamental questions, including the relative significance of different nonlinear absorption processes, is still lacking. The relative role of photoionization processes depends on material properties and on the laser pulse duration and wavelength.

In our previous work,[7] we investigated effects of high-power midinfrared (MIR) laser pulses on a bulk germanium (Ge) crystal using a free-electron laser (FEL). We measured optical transmittance through Ge for $\lambda=5.3-12.4$ μm at room temperature. In spite of the fact that Ge is transparent in the MIR region, we observed strong suppression of optical transmission under high-intensity FEL excitation. We found that the observed suppression was due to FEL-induced optical absorption in Ge because both transmission and reflection powers decreased simultaneously as the FEL power increased. To explain the mechanism of the FEL-induced absorption, we proposed band-to-band absorption process based on the Keldysh theory[8] which assumes oscillatory motion of the Bloch electron driven by intense fields. We calculated the transmittance of Ge within the Keldysh theory and found that the results were in reasonable agreement with the experimental results. However, there was also a possibility of interband impact ionization induced by residual free carriers accelerated by intense FEL fields. Impact ionization initiated by these carriers might induce significant population of free carriers. Consequently, the large number of free carriers might cause the FEL-induced absorption. The detailed discussion of free-carrier absorption process was not possible from the previous experiments. This effect can be checked by studying temperature dependence of the FEL-induced absorption because the carrier concentration of semiconductors strongly depends on temperature. In the present study, we have measured temperature dependence of the transmittance of Ge to clarify the mechanisms of the FEL-induced absorption.

The plan of the paper is the following. In Sec. II, we will explain the measurement setup. In Sec. III, we will present the experimental results. First, we will show the temperature dependence of the transmission spectra. Second, we will show the wavelength and irradiation power dependence of the transmission spectra at $T=11$, 100, 200, and 300 K. In Sec. IV, we will present the theoretical results and compare them with the experimental results. A summary is given in Sec. V.

II. EXPERIMENTAL METHOD

Figure 1 shows a schematic diagram of the measurement setup. A detailed discussion of the measurement setup can be found in Ref. 7 and we will briefly explain it for the sake of completeness.

The MIR FEL beam (pulse width: 5 ps) was focused on a sample by a ZnSe lens of 80 mm in diameter. The sample is a 3-mm-thick bulk Ge crystal. It was put into a cryostat with ZnSe windows. In the present experiments, the sample was heated with a heater in the cryostat. Temperature was controlled between 11 and 300 K using the heater and a temperature controller. A polarizer was located between the ZnSe lens and the sample for adjusting the irradiation power. The average power P_{av} was measured by a power meter. Since FEL wave forms suffer from distortion,[7] we measured temporal variation of the transmission using a mercury cadmium telluride MIR detector and a digital oscilloscope. We measured wavelength and FEL-power dependence of the

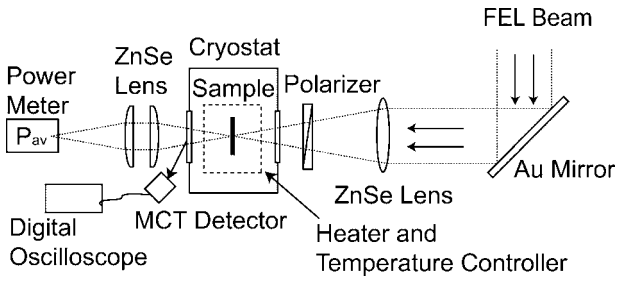

FIG. 1. A schematic diagram of the measurement setup.

 ©2007 The American Physical Society

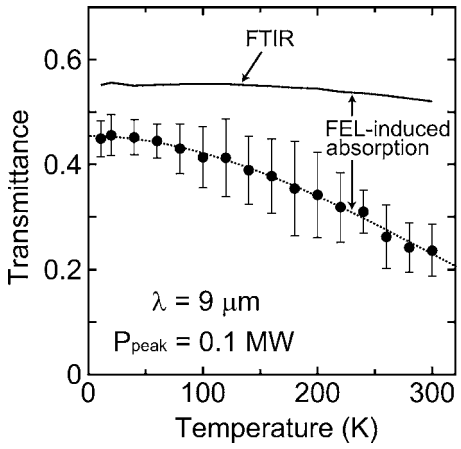

FIG. 2. Temperature dependence of the transmittance of a 3-mm-thick Ge sample at about 20 K intervals for $\lambda=9$ μm and $P_{\text{peak}}=0.1$ MW. The solid circles show the transmittance measured with the FEL. The error bars represent the standard deviations of the measurements. The dashed line is a guide to the eye. The solid line shows the transmittance measured by FTIR absorption spectroscopy. The difference between the FEL transmittance and the FTIR transmittance corresponds to the FEL-induced absorption.

transmittance of Ge for $\lambda=5.3-12.4$ μm at about 0.3 μm intervals and for $T=11-300$ K at 20 K intervals. We also carried out measurements using a Fourier transform infrared (FTIR) spectrometer at various temperatures. Note that the results of the FTIR measurements correspond to the low-field transmittance.

III. EXPERIMENTAL RESULTS

The time-resolved signal and the average power (P_{av}) were used to evaluate the peak power of the incident FEL beam (P_{peak}) and that of the transmitted beam.[7] The transmittance was calculated from their ratio. The solid circles in Fig. 2 show temperature dependence of the transmittance of Ge for $\lambda=9$ μm and $P_{\text{peak}}=0.1$ MW. The error bars represent the standard deviations of the measurements. The solid line in Fig. 2 shows the transmittance measured by FTIR absorption spectroscopy. As can be seen in Fig. 2, the transmittance measured with the FEL increases as temperature decreases. On the other hand, the transmittance measured by FTIR absorption spectroscopy depends rather weakly on temperature. The FEL-induced absorption reported in our previous paper[7] is determined by the difference between the FEL transmittance and the FTIR transmittance. Figure 2 clearly shows that the FEL-induced absorption decreases as temperature decreases.

To study this effect in more detail, we measured wavelength λ and FEL-power P_{peak} dependence of the transmittance of Ge for various temperatures. Figures 3(a)–3(d) show λ and P_{peak} dependences of the transmittance of Ge at $T=300$, 200, 100, and 11 K, respectively. The surfaces are generated by interpolation between data points. The solid circles with an arrow indicate the points for $\lambda=9$ μm and $P_{\text{peak}}=0.1$ MW. They correspond to the data points in Fig. 2. In Figs. 3(a)–3(d), we also plot the FTIR transmittance spectra for each temperature by solid lines. As can be seen in Fig. 3(a), the transmittance at 300 K is strongly suppressed as P_{peak} increases when $P_{\text{peak}}<0.1$ MW. For $P_{\text{peak}}>0.1$ MW,

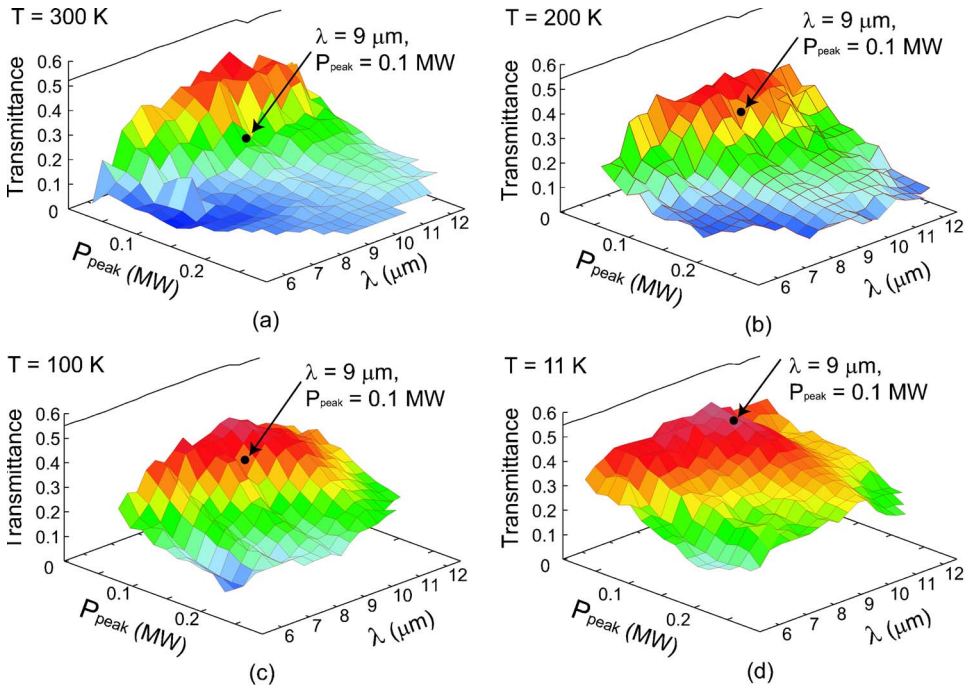

FIG. 3. (Color online) Transmittance of a 3-mm-thick Ge sample as a function of the FEL wavelength λ and the FEL peak power P_{peak} at (a) $T=300$ K, (b) $T=200$ K, (c) $T=100$ K, and (d) $T=11$ K. The surfaces are generated by interpolation between data points. The circles with an arrow indicate the points for $\lambda=9$ μm and $P_{\text{peak}}=0.1$ MW. The solid lines show the FTIR transmission spectra.

the transmittance was converged to ~0.1. The convergence of the experimental transmittance might be due to laser ablation because we have often observed laser damage to the surface of Ge when the transmittance was less than 0.1. In Figs. 3(b) and 3(c), the transmittance at $T=200$ and 100 K are also suppressed as P_{peak} increases. However, the suppression of the transmittance for $P_{peak}<0.1$ MW is not strong as compared to the results at 300 K. In Fig. 3(d), the transmittance is weakly suppressed as P_{peak} increases except for $\lambda \sim 10$ μm, where the transmittance hardly depends on P_{peak}. The overall suppression of the transmittance is found to become weaker with decreasing temperature.

IV. DISCUSSION

In the following, we examine the validity of two different absorption processes for the FEL-induced absorption. First, we focus on the band-to-band absorption process based on the Keldysh theory.[8] In the limiting case of low frequencies and strong electric fields, the conduction-band electrons are generated by tunneling ionization (TI). However, at high frequencies, there should appear a frequency dependence of the tunneling probability because the frequency of the electric field ω becomes larger than tunneling frequency $\omega_t = eF/(mE_g)^{1/2}$ and the electron does not have time to jump through the barrier within one cycle, and multiphoton ionization (MPI) occurs for $\omega \gg \omega_t$. Here, E_g is the band-gap energy, F is the electric field intensity, e is the elementary charge, and m is the electron effective mass. For atoms and semiconductors in intense fields, these photoionization processes can be treated under the same theoretical framework based on the Keldysh theory. Whether TI or MPI dominates, the excitation process is determined by the Keldysh parameter γ, defined as

$$\gamma = \frac{\omega}{\omega_t} = \frac{\omega(mE_g)^{1/2}}{eF}. \quad (1)$$

In our case, we estimate ω_t to be about 2.4×10^{14} s^{-1} when $F=1$ MV/cm. Note that $m=0.034m_0$ and $E_g=0.90$ eV, the direct energy gap of Ge, were used.[9] This corresponds to the frequencies of the MIR FEL fields. Therefore, this work is the case of $\gamma \sim 1$ which corresponds to the transition between the classical and quantum regimes. In this region, the photoionization process can be described neither by the usual formula for MPI at high frequency and not very strong fields[4] ($\gamma \gg 1$) nor by the usual formula for TI at low frequency and very strong fields[5] ($\gamma \ll 1$). Therefore, we have calculated the photoionization probability via the Keldysh theory. In the present study, we considered the temperature dependence of the direct-gap energy of Ge. A detailed derivation of the probability of the direct transition from the valence band to the conduction band can be found in Refs. 7 and 8 and we will briefly explain the formalism for completeness. Keldysh derived a formula for the probability of transition not to a stationary final state but to a state of the accelerated electron in an electric field $F(t)=F\cos\omega t$. The probability W_0 of the direct transition from the valence band to the conduction band per unit volume can be written as

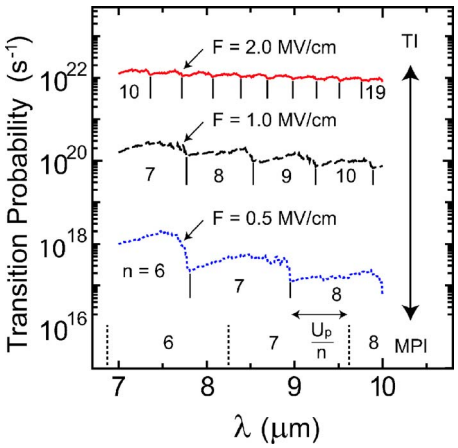

FIG. 4. (Color online) Calculated transition probability for various electric fields for $E_g=0.90$ eV. This figure represents the crossover from tunneling ionization (TI) to multiphoton ionization (MPI) behavior. The red solid line, black dashed line, and blue dotted line represent the calculated results for $F=2.0$, 1.0, and 0.5 MV/cm, respectively. The numbers below the transition probability n represent the smallest integers not less than or equal to $\bar{\varepsilon}_{cv}(\boldsymbol{k})/\hbar\omega$. For comparison, we have also shown the numbers of the case for $\bar{\varepsilon}_{cv}(\boldsymbol{k})=E_g$, which corresponds to the case of $F=0$ MV/cm, in the lowest part. The boundary positions shift to higher energies with increasing F. The amounts of the energy shifts are given by U_p/n. The transition probability strongly depends on the frequency and behaves like MPI at $F=0.5$ MV/cm. However, the frequency dependence becomes weaker as F increases, and the transition probability behaves like TI at $F=2.0$ MV/cm.

$$W_0 = \frac{2\pi}{\hbar}\left(\frac{eF}{2m\omega}\right)^2 P_{cv}^2 \sum_n \sum_{\boldsymbol{k}} |\mathcal{L}_n(\boldsymbol{k})|^2 \delta[\bar{\varepsilon}_{cv}(\boldsymbol{k}) - n\hbar\omega], \quad (2)$$

where P_{cv} is the momentum matrix element,

$$\mathcal{L}_n(\boldsymbol{k}) = \frac{1}{\pi}\int_{-\pi}^{\pi} \exp\left\{ i\frac{n}{\bar{\varepsilon}_{cv}(\boldsymbol{k})}\int_0^{\theta} \varepsilon_{cv}[\boldsymbol{k}(\phi/\omega)]d\phi \right\} \cos\theta d\theta, \quad (3)$$

and $\bar{\varepsilon}_{cv}(\boldsymbol{k})$ denotes the average energy gap between valence and conduction bands $\varepsilon_{cv}(\boldsymbol{k})$ per cycle in alternating electric fields can be written as

$$\bar{\varepsilon}_{cv}(\boldsymbol{k}) = \frac{1}{2\pi}\int_{-\pi}^{\pi} \varepsilon_{cv}[\boldsymbol{k}(\theta/\omega)]d\theta. \quad (4)$$

The effective threshold energy of absorption $\bar{\varepsilon}_{cv}(\boldsymbol{k})$ exceeds the band-gap energy E_g by the average oscillation energy of the electron in the field of the wave, i.e., the ponderomotive energy $U_p=e^2F^2/4m\omega^2$. This is precisely the quantity which enters into the δ function expressing the energy conservation law in Eq. (2). The formula also has the explicit form of the sum of multiphoton processes. Therefore, the Keldysh theory comprises a generalization of the theory of TI to include MPI in crystalline materials in the presence of strong alternating fields. In Fig. 4, we show an example of calculated transition probability for various electric fields when $E_g=0.90$ eV. Figure 4 represents the crossover from TI to MPI behavior. The

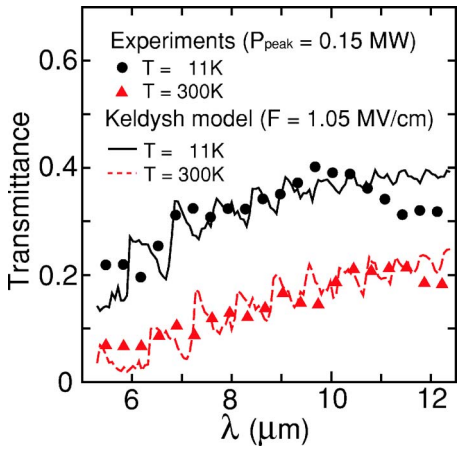

FIG. 5. (Color online) Transmittance of a 3-mm-thick Ge sample as a function of the wavelength λ including both theoretical and experimental results. The solid and dashed lines represent the calculated results for $T=11$ and 300 K when $F=1.05$ MV/cm, respectively. The solid circles and solid triangles represent the experimental results for $T=11$ and 300 K when $P_{\text{peak}}=0.15$ MW, respectively.

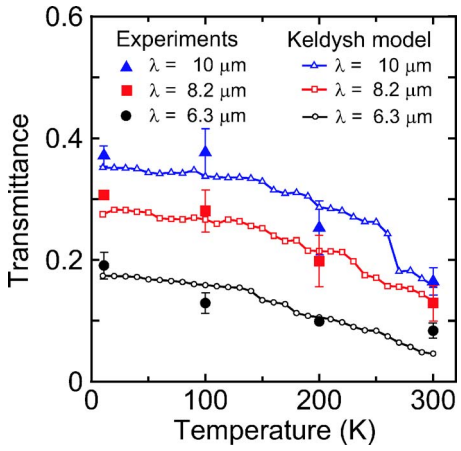

FIG. 6. (Color online) Transmittance of a 3-mm-thick Ge sample as a function of the temperature including both theoretical and experimental results. The solid circles, solid squares, and solid triangles represent the experimental results for λ=6.3, 8.2, and 10 μm, respectively, when $P_{\text{peak}}=0.15$ MW. The error bars represent the standard deviations of the measurements. The open circles, open squares, and open triangles represent the calculated results for λ=6.3 μm and $F=1.12$ MV/cm, λ=8.2 μm and $F=1.07$ MV/cm, and λ=10 μm and $F=1.06$ MV/cm, respectively.

solid line, dashed line, and dotted line represent the calculated results for $F=2.0$, 1.0, and 0.5 MV/cm, respectively. For λ=8 μm, γ are 0.49, 0.98, and 1.97 when $F=2.0$, 1.0, and 0.5 MV/cm, respectively. In Fig. 4, the numbers below the transition probability n represent smallest integers not less than or equal to $\bar{\varepsilon}_{cv}(\boldsymbol{k})/\hbar\omega$. For comparison, we have also shown the numbers of the case for $\bar{\varepsilon}_{cv}(\boldsymbol{k})=E_g$, which corresponds to the case of $F=0$ MV/cm, in the lowest part of Fig. 4. As can be seen in Fig. 4, the boundary positions shift to higher energies with increasing F. The amounts of the energy shifts are given by U_p/n, as shown in Fig. 4. The transition probability strongly depends on the frequency and behaves like MPI at $F=0.5$ MV/cm. However, the frequency dependence becomes weaker as F increases, and the transition probability behaves like TI at $F=2.0$ MV/cm.

The transition probability per unit volume W_0 was used to evaluate a complex dielectric function. The complex dielectric function was used to estimate an absorption coefficient. By neglecting Fabry-Pérot-type interference between surfaces, the transmittance of Ge T_{Ge} can be obtained using the absorption coefficient.[7] In the present paper, the following empirical expression given by Varshni is used to describe the temperature dependence of the energy gap:[10]

$$E_g = E_0 - \frac{\alpha T^2}{T+\beta}, \tag{5}$$

where E_0 is the energy gap at $T=0$ K. We used the following parameters in the calculations: $\alpha=7.25\times10^{-4}$ eV/K, $\beta=433$ K, $E_0=0.90$ eV, $m=0.034m_0$, and $P_{cv}=1.36$ a.u.[9,11,12]

In Fig. 5, we show the wavelength dependence of the transmittance of Ge calculated using the Keldysh theory at $F=1.05$ MV/cm. The solid and dashed lines represent the calculated results at $T=11$ and 300 K, respectively. In Fig. 5, we also plot the experimental results. The solid circles and triangles represent the experimental results for $P_{\text{peak}}=0.15$ MW at $T=11$ and 300 K, respectively. These are obtained from Figs. 3(a) and 3(d). As can be seen in Fig. 5, the calculated results are in reasonable agreement with the experimental results, apart from the oscillatory behavior appearing in the calculated results. The oscillatory behavior is caused by the contribution of MPI, which becomes significant when γ is further increased. As can be seen in the calculated results for $T=11$ K, the oscillatory behavior becomes larger with decreasing λ. At $F=1.05$ MV/cm and $T=11$ K, we estimate the Keldysh parameters γ to be 1.25 for λ=6 μm and 0.62 for λ=12 μm.

Shown in Fig. 6 is the transmittance of Ge as a function of the temperature including both experimental and theoretical results. The solid circles, solid squares, and solid triangles represent the experimental results for $P_{\text{peak}}=0.15$ MW and λ=6.3, 8.2, and 10 μm, respectively. The open circles, open squares, and open triangles represent the calculated results. Note that the focused beam spot sizes D were adjusted in the calculations to fit with the experimental results by using the least-squares method, since the actual focused beam spot sizes are unclear only from the experimental conditions. The electric-field strength F was obtained from the focused beam spot sizes D and the peak power P. The peak power at the sample P is estimated to be 0.38 MW when the FEL peak power at the power meter $P_{\text{peak}}=0.15$ MW by considering the absorption of the ZnSe window and lenses. The parameters used in the calculations have been listed in Table I. We have also listed the diffraction limited spot sizes D^*, together with the typical diameter d and focal lengths l of the ZnSe lens used in the present experiments. As can be seen in Table I, the focused beam spot sizes D obtained by fitting the experimental data are slightly larger than the diffraction limited spot sizes D^* for all wavelengths, which are consistent with physical intuition. In Fig. 6, we obtained reasonable agreement between the experimental results and the Keldysh

TABLE I. Focused beam spot sizes D and diffraction limited spot sizes D^* of each wavelength.

λ (μm)	P^a (MW)	F^b (MV/cm)	D (μm)	d^c (mm)	l^d (mm)	D^* (μm)
6.3	0.38	1.12	85.2	80	376	37.7
8.2	0.38	1.07	89.2	80	378	49.3
10	0.38	1.06	92.7	80	380	60.5

[a]Peak power at the sample when $P_{peak}=0.15$ MW.
[b]Electric-field strength obtained from P and D.
[c]Diameter of the ZnSe lens.
[d]Focal lengths of the ZnSe lens.

theory. Therefore, we concluded that the Keldysh theory can explain the observed FEL-induced absorption. Note that a sudden variation of the calculated transmittance for $\lambda=10$ μm has been observed in Fig. 6 at $T\sim 250$ K. This is because while the terms of $n\geqslant 10$ in Eq. (2) contribute to the transition when $T\gtrsim 250$ K, the term of $n=10$ cannot involve the transition when $T\lesssim 250$ K due to the band-gap widening at lower temperatures.

Second, we concentrate on the free carrier absorption (FCA) process. There is a possibility of interband impact ionization induced by residual free electrons accelerated by intense FEL fields beyond the threshold energy of impact ionization. The accelerated electrons eventually lose some of their energy through the impact ionization process creating electron-hole pairs. Integrated number of occurrence of impact ionization in GaAs has been calculated by a full-band Monte Carlo simulation as a function of time for MIR FEL pulses of wavelengths $\lambda=9.8$ and 7.1 μm for $F=1$ MV/cm at $T=10$ K.[13] In that work, scattering-induced electron heating was a quite fast process and a number of impact ionization occurrences can be seen already at 1 ps (see Fig. 3 in Ref. 13). However, the integrated number of occurrences of impact ionization was estimated to be less than 20% of the number of the initial electrons in 3 ps when $\lambda=9.8$ μm and $F=1$ MV/cm, which means that the avalanche ionization would not happen during the FEL micropulse (5 ps). Therefore, the possibility of the FCA is expected to strongly depend on the initial free-carrier concentration of Ge. The intrinsic carrier concentration of Ge n_i (per cubic centimeter) can be estimated as

$$n_i = 1.76 \times 10^{16} T^{3/2} \exp(-0.785/2kT), \tag{6}$$

where T is the temperature in kelvins and k is the Boltzmann constant in eV/K.[9] The carrier concentrations for $T=30$ and 300 K are estimated to be 3.35×10^{-48} and 2.33×10^{13} cm^{-3}, respectively. The carrier concentration of Ge greatly depends on temperature. This is too large to explain the observed temperature dependence of the FEL-induced absorption. Therefore, we exclude the FCA process for the FEL-induced absorption process.

Note that we have observed that the transmittance decreases with λ for $\lambda>10$ μm at $T=11$ K (see Fig. 5). The observed decrease may originate from impurity absorption because it occurs only at very low temperatures. However, a complete view of this decrease for $\lambda>10$ μm is still lacking. The reason for this is under investigation.

V. SUMMARY

In summary, we investigated the temperature dependence of MIR FEL-induced absorption spectra of Ge in intense laser fields. We found that the FEL-induced absorption decreases as temperature decreases. The theoretical results using the Keldysh theory by considering the temperature dependence of direct-gap energy of Ge are in reasonable agreement with the experimental results. We concluded that the Keldysh theory can explain the FEL-induced absorption.

[1] S. Guizard, A. Semerok, J. Gaudin, M. Hashida, P. Martin, and F. Quéré, Appl. Surf. Sci. **186**, 364 (2002).
[2] P. G. Eliseev, O. N. Krokhin, and I. N. Zavestovskaya, Appl. Surf. Sci. **248**, 313 (2005).
[3] M. D. Feit, A. M. Komashko, and A. M. Rubenchik, Appl. Phys. A: Mater. Sci. Process. **79**, 1657 (2004).
[4] V. Nathan, A. H. Guenther, and S. S. Mitra, J. Opt. Soc. Am. B **2**, 294 (1985).
[5] C. Zener, Proc. R. Soc. London, Ser. A **145**, 532 (1934).
[6] B. C. Stuart, M. D. Feit, A. M. Rubenchik, B. W. Shore, and M. D. Perry, Phys. Rev. Lett. **74**, 2248 (1995).
[7] H. Furuse, N. Mori, H. Kubo, H. Momose, and M. Kondow, Phys. Rev. B **74**, 205206 (2006).
[8] L. V. Keldysh, Sov. Phys. JETP **20**, 1307 (1965).
[9] O. Madelung, *Semiconductors: Data Handbook*, 3rd ed. (Springer-Verlag, Berlin, 2004).
[10] Y. P. Varshni, Physica (Amsterdam) **34**, 149 (1967).
[11] P. A. Dafesh and K. L. Wang, Phys. Rev. B **45**, 1712 (1992).
[12] C. Hamaguchi, *Basic Semiconductor Physics* (Springer-Verlag, Berlin, 2001).
[13] N. Mori, H. Nakano, H. Kubo, C. Hamaguchi, and L. Eaves, Physica B **272**, 431 (1999).